

Structure evolution of zinc oxide thin films deposited by unbalance DC magnetron sputtering

Didik Aryanto, Putut Marwoto, Toto Sudiro, Muhammad D. Birowosuto, Sugianto, and Sulhadi

Citation: [AIP Conference Proceedings](#) **1729**, 020039 (2016); doi: 10.1063/1.4946942

View online: <http://dx.doi.org/10.1063/1.4946942>

View Table of Contents: <http://scitation.aip.org/content/aip/proceeding/aipcp/1729?ver=pdfcov>

Published by the [AIP Publishing](#)

Articles you may be interested in

[Structural and optical properties of DC reactive magnetron sputtered zinc aluminum oxide thin films](#)

[AIP Conf. Proc.](#) **1620**, 118 (2014); 10.1063/1.4898229

[Morphology and structure evolution of tin-doped indium oxide thin films deposited by radio-frequency magnetron sputtering: The role of the sputtering atmosphere](#)

[J. Appl. Phys.](#) **115**, 154905 (2014); 10.1063/1.4871810

[Effect of film thickness on surface morphology and optical properties of nanostructured Zinc Aluminum Oxide thin films deposited by DC magnetron sputtering](#)

[AIP Conf. Proc.](#) **1451**, 200 (2012); 10.1063/1.4732414

[Effect of Substrate Temperature on Optical Properties of Aluminum Zinc Oxide Thin Films Deposited by DC Magnetron Sputtering](#)

[AIP Conf. Proc.](#) **1391**, 167 (2011); 10.1063/1.3646813

[Deposition of aluminum-doped zinc oxide thin films for optical applications using rf and dc magnetron sputter deposition](#)

[J. Vac. Sci. Technol. A](#) **28**, 515 (2010); 10.1116/1.3425640

Structure Evolution of Zinc Oxide Thin Films Deposited by Unbalance DC Magnetron Sputtering

Didik Aryanto^{1,3,a)}, Putut Marwoto^{2,3}, Toto Sudiro¹, Muhammad D. Birowosuto^{1,4},
Sugianto^{2,3} and Sulhadi²

¹Research Center for Physics, Indonesian Institute of Sciences, Serpong 15314, Tangerang Selatan, Indonesia

²Physics Department, Faculty of Mathematics and Science, Universitas Negeri Semarang

³Materials Research Group, Physics Department, Universitas Negeri Semarang,
Gunungpati, Semarang 50229 Jawa Tengah, Indonesia

⁴CINTRA UMI CNRS/NTU/THALES 3288 Research Techno Plaza, 50 Nanyang Drive, Border X Block, level 6,
637553, Singapore

^{a)}Corresponding author: didi027@lipi.go.id

Abstract. Zinc oxide (ZnO) thin films are deposited on corning glass substrates using unbalanced DC magnetron sputtering. The effect of growth temperature on surface morphology and crystallographic orientation of ZnO thin film is studied using atomic force microscopy (AFM) and X-ray diffraction (XRD) techniques. The surface morphology and crystallographic orientation of ZnO thin film are transformed against the increasing of growth temperature. The mean grain size of film and the surface roughness are inversely and directly proportional towards the growth temperature from room temperature to 300 °C, respectively. The smaller grain size and finer roughness of ZnO thin film are obtained at growth temperature of 400 °C. The result of AFM analysis is in good agreement with the result of XRD analysis. ZnO thin films deposited in a series of growth temperatures have hexagonal wurtzite polycrystalline structures and they exhibit transformations in the crystallographic orientation. The results in this study reveal that the growth temperature strongly influences the surface morphology and crystallographic orientation of ZnO thin film.

INTRODUCTION

ZnO is one of metal-oxide with direct band gap of 3.37 eV with a large exciton binding energy of 60 eV at room temperature [1, 2]. Since 1960s, ZnO thin films have been extensively investigated because of their optical transparency, high reflection constant, large piezoelectric constant and ultraviolet (UV) emission properties. In addition to their low cost, non-toxic and relatively low deposition temperature, high chemical stability in reduction environments and stability in hydrogen plasma compared to ITO and SnO₂ [3]. They become the promising alternatives to indium tin oxide (ITO) films in transparent conducting oxide (TCO) applications.

In recent years, lots of studies were concentrated on the TCO based on ZnO thin films for thin film (silicon) solar cells. In solar cells, TCO layers functionalized as electrodes which can transmit and scatter light into photovoltaic cells [4]. Therefore, the lower the resistivity, the transmittance in the wavelength of visible-near-infrared (350-900 nm) will be higher and the certain surface roughness are the essential properties for the photovoltaic cells. Hong *et al.* [5] show that the roughness surface morphology of ZnO thin film affects the transmission and the absorption. Additionally, the resistivity of Al-doped ZnO thin film also depends on the grain size and the surface morphology [6]. Rao and Santhoshkumar [7] also demonstrated that the grain size and structure of the film did not solely contribute to the optical properties of ZnO thin film but also the electrical properties. In the fabrication of thin film silicon solar cell, the structure and surface morphology of ZnO thin film affects the structure of silicon layers. On one side, Calgar *et al.* [4] showed that the structure of thin film silicon solar cell is influenced by the surface roughness of TCO (nanocrystalline ZnO) while it has contributions in the open circuit voltage (*V_{oc}*)

and fill factor (FF) in tandem cell. On the other hand, the texture surfaces of Al-doped ZnO domain determine the short-circuit current density (J_{sc}) of the cell device [8]. Therefore, elaboration to the previous studies, the structural and morphological of ZnO thin film are very important when TCO is embedded inside the thin film solar cell.

ZnO thin films were usually grown by several deposition methods, such as DC and RF magnetron sputtering, pulsed laser deposition (PLD), metal-organic chemical vapor deposition (MOCVD), molecular beam epitaxy (MBE), spray pyrolysis and sol-gel technique. In this study, we use a homemade “unbalanced DC magnetron sputtering” for the deposition of ZnO thin film. Our previous works demonstrated a successful deposition of the pristine oxide thin film using the similar methods [9-11]. In this work, the morphological and structural evolutions of ZnO thin film due to the influence of growth temperature using AFM and XRD characterizations will be investigated.

EXPERIMENTAL

ZnO thin films were deposited on corning glass substrate ($10 \times 10 \text{ mm}^2$) using homemade unbalanced DC magnetron sputtering. For ZnO thin film deposition, 99.999% purity ZnO target was used. The glass substrate was cleaned in an ultrasonic bath with acetone (10 min) and methanol (5 min), and then cleaned with deionized water. Further, the substrate was dried using O_2 gun, and mounted in the sputtering chamber. Prior to the ZnO thin film deposition, the target was pre-sputtered for 10 min to remove contaminant from the surface. The chamber was initially evacuated to a base pressure of 1×10^{-4} Torr, and the deposition was carried out at a working pressure of 5×10^{-1} Torr. High-purity (99.999%) Ar gas was applied as plasma source. The DC power on target was maintained at 40 W, and the distance between the target and the substrate was set at 45 mm. The ZnO thin films were deposited at four different substrate temperatures of 27 (room temperature ‘RT’), 200 °C, 300 °C and 400 °C. The crystallinity of ZnO thin films were analyzed by using an XRD instrument equipped with a Cu-source ($\lambda = 1.5406 \text{ \AA}$). The AFM characterization was employed to investigate the surface morphology and root-mean-square (rms) roughness of thin film.

RESULTS AND DISCUSSION

The XRD patterns of ZnO thin films with a series of growth temperatures are shown in Fig. 1. The XRD studies revealed that all ZnO thin films exhibit a polycrystalline with a hexagonal structure of the wurtzite-type. In Fig. 1, the ZnO thin film carries a high preferential orientation along the (002) plane. Other diffraction peaks, (100), (101), and (110), with less intensity were also observed. It indicates the ZnO thin film exhibits a strong c -axis orientation perpendicular to the substrate. The texture coefficient (TC), which is calculated using the following equation, may explain the preferential random growth of polycrystalline thin film [12].

$$TC = \left(\frac{I_{(hkl)} / I_{r(hkl)}}{\left[\frac{1}{n} \sum I_{(hkl)} / I_{r(hkl)} \right]} \right) \quad (1)$$

where $I(hkl)$ is the XRD intensity from the thin film, n is the number of reflections observed in the XRD pattern, and $I_r(hkl)$ is the intensity of the reference (ICDD-01-078-3315). The value of the texture coefficient indicates the maximum preferred orientation of the films along the diffraction plane [12, 13]. Data of the variation of the texture coefficient against a series of growth temperature for the (002) plane is displayed in Table 1. All ZnO thin film have a relatively higher value of texture coefficient (>1) along the (002) plane. Rao and Santhoshkumar [12] have observed the same results and therefore, we may conclude that the crystallites are preferentially oriented along the (002) plane. From the definition of texture coefficient, it can be explained that the increase in preferred orientation can be associated with increase of the number of grains along that plane. In this study, the increase of texture coefficient value is associated with the increase of the number of grains along (002). Figure 1 also shows that the intensity of the (002) diffraction peak increases when the growth temperature increases from 27 °C to 300 °C while other peaks simultaneously decreases. It indicates that the crystalline quality of the ZnO thin films was improved during the growth. The peak intensities at (002) plane decrease at the growth temperature of 400 °C. The different of XRD peak intensity in ZnO thin film is related to the grain and crystalline sizes of the films. The XRD peak intensities decrease along with the decrease of the grain and crystalline sizes. In the earlier observation, Li *et al.*, [14] attributed the intensity decrease to the miss-orientation of (002) planes with the substrate surface. A small shift

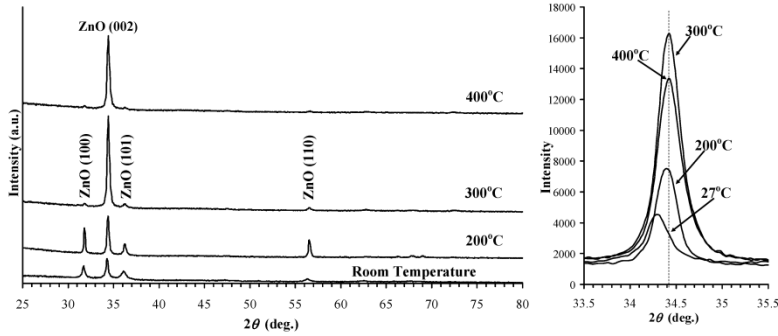


FIGURE 1. XRD patterns of ZnO thin films grown at different substrate temperatures

TABLE 1. Calculated d-spacing, FWHM, Crystalline size, lattice strain, dislocation density, and lattice constants of ZnO (002) thin films growth at various substrate temperatures

Substrate temperature	TC	d-spacing [Å]	FWHM	Crystalline size [Å]	Lattice strain (ϵ) [%]	ρ (line/nm ²) $\times 10^{-2}$	c [Å]
27 °C (RT)	1.814	2.6133	0.28	5.18674	0.2267	0.0579	5.2265
200 °C	1.643	2.6092	0.28	5.18752	0.2263	0.0579	5.2183
300 °C	3.164	2.6051	0.28	5.18829	0.2260	0.0579	5.2102
400 °C	3.130	2.6051	0.30	4.84241	0.2421	0.0665	5.2102

towards greater angles is showed on the position of (002) peak in Fig. 1. It suggests a decrease of the c -lattice parameter of ZnO [15] and possibly relates to the strain relaxation in the films [16]. The XRD spectra have the same values of full width at half maximum (FWHM) at (002) plane of 0.28° when the growth temperature increase from 27 °C to 300 °C. At 400 °C, the values of FWHM increase to 0.30°. These values are associated with the crystalline size, lattice strain and dislocation densities.

The average size (D) of the crystalline grain along the c -axis is determined using Debye-Scherrer's formula [12, 13]:

$$D = \frac{0.9 \lambda}{\beta \cos \theta} \quad (2)$$

where λ is the X-ray wavelength of 1.5418 Å, θ is Bragg diffraction angle of the (002) peak and β is the FWHM of θ . The crystalline size of the ZnO thin film growth at different temperatures is tabulated in the Table 1. Increasing the growth temperature from room temperature to 300 °C resulted in a slight increase of the crystalline size of ZnO thin film. The crystallites are increased due to the merging process of small crystallite as the temperature effect. However, the crystalline size considerably decreases at the growth temperature of 400 °C. This is due to the speed increase of atoms deposited on the substrate. Atoms do not have enough time to migrate and diffuse at the substrate surface. It is caused by the collision with other atoms during deposition, which induces lattice strain in the films. The lattice strain (ϵ) was calculated using the tangent formula [17]

$$\epsilon = \frac{\beta}{(4 \tan \theta)} \quad (3)$$

Lattice strain affects the length of the dislocation lines per unit volume of the crystal. Dislocation density (ρ) due to lattice strain can be expressed by the relation [12]

$$\rho = \left[\frac{\sqrt{12} \epsilon}{D d} \right] \quad (4)$$

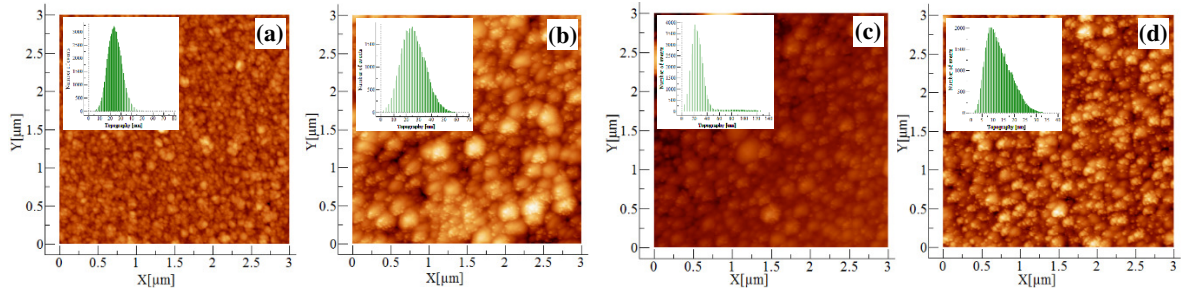


FIGURE 2. AFM images and topographic profiles of ZnO thin films grown at the growth temperatures of 27 °C (RT), 200 °C, 300 °C and 400 °C, respectively

where d is the d -spacing of different crystal planes, which is determined using the equation [17]

$$\frac{1}{d^2} = \frac{4(h^2 + hk + k^2)}{(3a^2)} + \left(\frac{l^2}{c^2}\right) \quad (5)$$

The calculated of d -spacing, lattice strain and dislocation density are presented in the Table 1. As shown in the Table 1, the value of lattice strain and dislocation densities decrease with the increase of the growth temperature, but slightly enhance at the growth temperature of 400 °C. It can be explained that the growth temperature in the sputtering system affects the kinetics energy of atom. High temperatures lead to an increase in the kinetic energy of the atoms.

Atoms are not regularly arranged when there is not enough time to migrate and diffuse. It causes the non-uniform displacement of the atoms with respect to their reference-lattice positions [18]. Another reason, the lattice strain and dislocation densities resulting from lattice mismatch between the substrate and film [19]. Increasing the lattice strain and dislocation density was promoted by the broadening on FWHM in the XRD pattern. Table 1 also shows that the growth temperature affects the lattice constant of the ZnO (002). In this study, the value is higher than theory ($c = 5.207 \text{ \AA}$ from ICDD-01078-3315) with the variation difference in the range of 0.003-0.020 Å. The increase in the lattice parameter is probably due to the presence of strain fields within the non-equilibrium grain boundaries inside of crystallite.

The AFM images and topographic profile of a $3 \times 3 \mu\text{m}^2$ scanning as function of various growth temperatures is displayed in Fig. 2. The surface morphologies of the films reveal a noticeable transformation with increasing growth temperature. The difference in the surface morphology can be explained as the contact angle is changed by varying the surface/interface energy of the films [20]. The root mean square (RMS) surface roughness values are 7.05 nm, 9.54 nm, 17.05 nm, and 5.67 nm for ZnO thin film with growth temperature of 27 °C, 200 °C, 300 °C and 400 °C, respectively. The changes in surface roughness are due to different in grain size deposited on the surface at different growth temperature. As shown in Fig. 2(c) and Fig. 2(d), the bigger grain size was formed on the surface and the surface roughness is higher than other samples. This result was confirmed by topographic profile. The larger grain is identified at the surface with the range size of 50-60 nm and 60-120 nm for ZnO thin film deposited at 200 °C and 300 °C, respectively. The larger grain formed on the surface when the growth temperature increases from 27 °C to 300 °C. The opposite result was demonstrated at the growth temperature of 400 °C. The grain becomes smaller (2-35 nm) and uniformly distributes throughout the surface. It causes the film to have a smooth surface compared to the other sample. In this case, the increasing growth temperature is in favor to the diffusion of atoms absorbed on the substrate and accelerates the migration of atoms to the favorable energy positions. As shown by Singh *et al.* [21] it causes the enhancement of the c -axis orientation of film. The result of AFM analysis is in good agreement with the XRD characterization.

CONCLUSIONS

ZnO thin film was successfully deposited on corning glass using unbalanced DC magnetron sputtering at various growth temperatures. Structural studies were conducted on ZnO thin film as the effect of the growth temperature. The XRD and AFM analysis of the films revealed a transformation on the structural and surface morphology of the

ZnO thin film with various growth temperatures. The ZnO thin film holds a high preferential orientation along the (002) plane with the increase of the growth temperature. The result of calculated d -spacing, FWHM, crystalline size, lattice strain, dislocation density, and lattice constants of ZnO (002) thin films promoted the occurrence of structural evolution. However, RMS surface roughness and grain size of ZnO thin film were also fluctuated with the increase of growth temperature. In the fabrication of ZnO thin films using sputtering system, structure and surface morphology of the films are strongly influenced by the growth temperature.

ACKNOWLEDGMENTS

This work was supported by Ministry of Education Republic of Indonesia under Grant No. 028/O06.2/PP/SP/2012. The authors are grateful to Laboratory of Thin Film, Physics Department, Faculty mathematics and natural sciences, Universitas Negeri Semarang and research center for physics-LIPI

REFERENCES

1. B. Cao, W. Cai, H. Zeng and G. Duan, *J. Appl. Phys.* **99**, 073516 (2006).
2. X. Z. Qiang, D. Hong, L. Yan and C. Hang, *Mater. Sci. Semicond. Process.* **9**, 132 (2006).
3. C. E. Kim *et al.*, *Thin Solid Films* **518**, 6304 (2010).
4. O. Caglar, P. Carroy, P. A. Losio and I. Sinicco, *Sol. Energ. Mat. Sol. C* **144**, 55 (2016).
5. C. S. Hong, H. H. Park, J. Moon and H. H. Park, *Thin Solid Films* **515**, 957 (2006).
6. G. X. Liang, P. Fan, X. M. Cai, D. P. Zhang and Z. H. Zheng, *J. Electron. Mater.* **40**, 267 (2011).
7. T. P. Rao and M. C. Santhoshkumar, *Appl. Surf. Sci.* **255**, 7212 (2009).
8. Q. Jiang *et al.*, *Sol. Energ. Mat. Sol. C* **130**, 264 (2014).
9. P. Marwoto, S. Sugianto and E. Wibowo, *J. Theor. App. Phys.* **6**, 17 (2012).
10. P. Marwoto *et al.*, *Adv. Mat. Res.* **896**, 237 (2014).
11. P. Marwoto *et al.*, *Adv. Mat. Res.* **1123**, 364 (2015).
12. T. P. Rao and M. C. Santhoshkumar, *J. Alloys Compd.* **506**, 788 (2010).
13. D. K. Kim and H. B. Kim, *Superlattices Microstruct.* **85**, 50 (2015).
14. X. Y. Li *et al.*, *Opt. Commun.* **282**, 247 (2009).
15. V. Khranovskyy *et al.*, *Superlattices Microstruct.* **42**, 379 (2007).
16. M. L. Cui, X. M. Wu, L. J. Zhuge and Y. D. Meng, *Vacuum* **81**, 899 (2007).
17. P. P. Sahay and R. K. Nath, *Sens. Actuators B Chem.* **134**, 654 (2008).
18. A. R. Bushroa, R. G. Rahbari, H. H. Masjuki and M. R. Muhamad, *Vacuum* **86**, 1107 (2012).
19. Z. Y. Zhai *et al.*, *J. Phys. D Appl. Phys.* **42**, 1 (2009).
20. K. U. Sim *et al.*, *Curr. Appl. Phys.* **10**, S463 (2010).
21. P. Singh, A. Kumar, Deepak and D. Kaur, *J. Cryst. Growth* **306**(2), 303 (2007).